$+ (i-1)d$ gives the distance across the face of the array. W_j denotes the weight matrix to the output layer in the jth training step. The received delay caused by geometrical paths in the absence of any delay noise is $\tilde{\tau}(x_i, z) = (x_i^2 + z^2)^{1/2}/c$, with c being the velocity. This velocity is used to compute the focusing delays in the beamformer. The delay noise τ_n is injected on the geometric delay function during the training of the network. In B-mode imaging the delay curvature itself changes with depth. The next task is to determine the training depths required for the network. A fixed fractional change in the geometrical delay curvature as an indicator of training depths was used. At distances closer to the array the delay curvature changes more rapidly, requiring closer training locations.

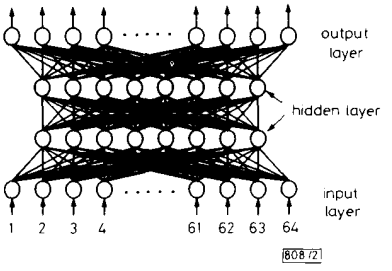

Fig. 2 *Neural network*

We have modelled the operations depicted in Fig. 1 for a 3·5 MHz imaging system with $N = 64$, $d = 0{\cdot}625$ mm and $l = 40$ mm, using $c = 1{\cdot}5$ mm/μs. The excitation waveform and aperture apodization functions were both Gaussian with 0·83 μs and 25·2 mm full width, respectively. We found that for this case, with a 1·5% change in the delay width and a maximum imaging depth of 240 mm, the network had to be trained at the depths of 10, 11, 13, 16, 19, 24, 32 and 57 mm. At each depth the network was trained 10 times by gradually varying the peak-to-peak delay noise from 0 to 100 ns (as compared to the wave period of 286 ns). Each training required an updating of the weight matrices up to 6000 times so that the relative error computed from eqn. 1 was less than 1%. The network produced satisfactory results at all depths

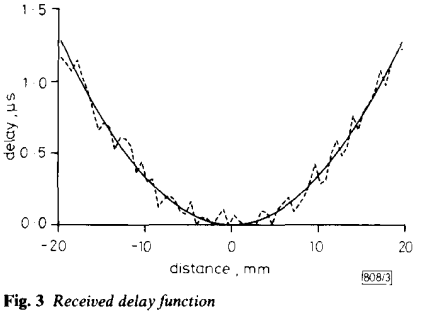

Fig. 3 *Received delay function*

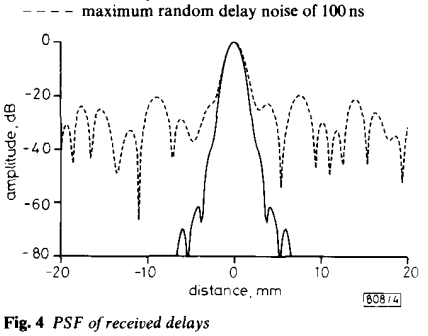

Fig. 4 *PSF of received delays*

for up to 240 mm once trained. The PSF at a depth of 100 mm which is not one of the training depths is presented. Fig. 3 shows the ideal and distorted echo delays across the array. In this case the peak-to-peak random delay noise is 100 ns. This noise function is different from any delay noise functions used during the training process. Fig. 4 shows the corresponding PSFs. We see that the sidelobes, which were below −60 dB for the ideal case, have risen to around −25 dB. The trained neural network was then used to correct the echo delays (dashed line in Fig. 3). The PSF obtained with the corrected delays is shown in Fig. 5. The improvement in the way of a substantial reduction in the sidelobe level is evident.

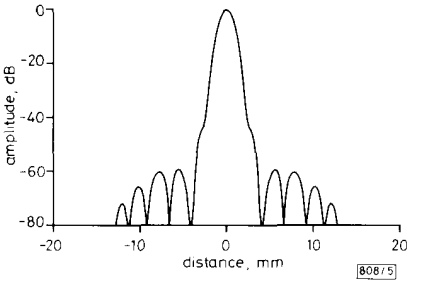

Fig. 5 *PSF after neural network correction*

In summary we have presented preliminary results on the application of neural networks to imaging in medical ultrasound and outlined a methodology for training the network. These results were obtained from software simulation of an imaging system. The hardware implementation of such a system and the optimisation of the neural network configuration/training is under investigation.

M. NIKOONAHAD

Siemens Ultrasound, 2527 Camino Ramon
San Ramon, CA 94583, USA

D. C. LIU

Bio-Imaging Research, Inc., 425 Barclay Boulevard
Lincolnshire, IL 60069, USA

19th February 1990

References

1 NIKOONAHAD, M.: 'Synthetic focused image reconstruction in the presence of a finite delay noise'. Proc. IEEE Ultrasonics Symposium, 1986, pp. 819–824
2 FLAX, S. W., and O'DONNELL, M.: 'Phase-aberration correction using signals from point reflectors and diffuse scatterers: basic principles', *IEEE Trans.*, 1988, **UFFC-35**, (6), pp. 758–767
3 NOCK, L., TRAHEY, G. E., and SMITH, S. W.: 'Phase aberration correction in medical ultrasound using speckle brightness as a quality factor', *J. Acoust. Soc. Am.*, 1989, **85**, (5), pp. 1819–1833
4 FINK, M., PRADA, C., and WU, F.: 'Self focusing with "time reversal" acoustic mirrors'. 'Acoustical imaging' Vol. 18, (Plenum), in press
5 CONRATH, B. C., DAFT, C. M. W., and O'BRIEN, W. D.: 'Applications of neural networks to ultrasound tomography'. Proc. IEEE Ultrasonics Symposium, 1989, in press
6 RUMEHART, D. E., HINTON, G. E., and WILLIAMS, R. J.: 'Learning internal representation by error propagation', *in* 'Parallel distributed processing' (MIT Press, Cambridge, MA, 1986), Vol. 1, pp. 318–362

COMMENT

BEHAVIOUR OF CIRCUIT-SWITCHED MULTISTAGE NETWORKS IN PRESENCE OF MEMORY HOT SPOT

Pombortsis and Halatsis have considered the behaviour of circuit switched multistage interconnection networks (MINs) in the presence of a memory hot spot.[3] An iterative algorithm was derived to compute the bandwidth of an n-stage MIN (each stage consists of α^{n-1} crossbar switching elements (SEs)

of size $\alpha \times \alpha$) under the hot spot nonuniform traffic. A closer look at the expressions for P_h^1 and P_{nh}^1 given in their letter reveals that each processor may independently generate at most two requests (one for the hot MM with probability rh and one for the uniform background with probability $r(1-h)$) in a network cycle. The number of requests received during a network cycle by an output link of a SE at each stage is one at most. The recursive formulas for P_h^i and P_{nh}^i when $i \geq 2$ should have different forms from those for P_h^1 and P_{nh}^1.

An alternative recursive algorithm to compute the bandwidths of MINs under the hot spot nonuniform traffic is presented. Suppose each processor can generate on request with probability r in a network cycle. A request is destined to the hot MM with probability $h + (1-h)/\alpha^n$ and to a regular MM with probability $(1-h)/\alpha^n$. Let $S(n; r, h)$ denote the throughput of an n-stage MIN under the above assumptions. Then we have

$$S(n; r, h) = S(n-1; r', h') + (\alpha - 1)S(n-1; r'', 0) \quad (1)$$

where

$$r' = 1 - \left[1 - rh - \frac{r(1-h)}{\alpha}\right]^{\alpha} \quad (2)$$

$$h' = \frac{\alpha h}{1 + (\alpha - 1)h} \quad (3)$$

$$r'' = 1 - \left[1 - \frac{r(1-h)}{\alpha}\right]^{\alpha} \quad (4)$$

Eqns. 2 and 4 can easily be derived. The expression for h' is now explained. Consider any hot port which is an output of an SE at stage 1. Let x_h and x_{nh} denote the probabilities that a request received by the hot port is destined to the hot MM and a regular MM reachable from the hot port, respectively. It is clear that x_h is equal to the probability that a request is destined to the hot MM provided it is destined to one of the MMs reachable from the hot port. After some calculations, we get $x_h = [h + (1-h)/N]/[h + (1-h)/\alpha]$ where $N = \alpha^n$. It can also be shown that $x_{nh} = [(1-h)/N]/[h + (1-h)/\alpha]$. The excess probability of the hot MM for a packet received by the hot port is equal to $h' = \alpha h/[1 + (\alpha - 1)h]$. Fig. 1 shows the BW (i.e. $S(n; 1, h)$) of MINs with $\alpha = 2$ for various values of excess probability h. It can be seen that the degradation of bandwidth is small for small values of h. A higher degree of nonuniformity results in a more serious degradation.

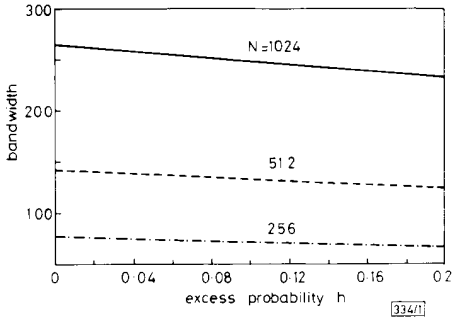

Fig. 1 *Bandwidth against probability for MINs*
$\alpha = 2$

A recursive algorithm for use when each processor can independently generate at most two requests can be similarly derived. Let β denote the probability that the request to the hot MM is selected and issued whenever two requests are generated simultaneously at a processor. Also, let $S^*(n; r, h)$ denote the throughput of an n-stage MIN under current assumptions.

$$S^*(n; r, h) = S(n-1; r', h') + (\alpha - 1)S(n-1; r'', 0) \quad (5)$$

where

$$r' = 1 - (1 - rh)^{\alpha}\left[1 - \frac{r(1-h)}{\alpha}\right]^{\alpha} \quad (6)$$

$$h' = \frac{\alpha\{rh[1 - r(1-h)] + rhr(1-h)\beta\}}{\alpha rh[1 - r(1-h)] + (1 - rh)r(1-h) + \alpha rhr(1-h)\beta + rhr(1-h)(1-\beta)} \quad (7)$$

$$r'' = 1 - \left[1 - \frac{r(1-h)}{\alpha}\right]^{\alpha} \quad (8)$$

Notice that $S(n; r, h)$ appeared in eqn. 5 can be computed by the recursive algorithm given in eqn. 1.

T.-H. LEE

Department of Communication Engineering
National Chiao Tung University
Hsinchu, Taiwan, Republic of China

28th November 1989

References

1 PRISTER, G. F., and NORTON, V. A.: '"Hot spot" contention and combining in multistage interconnection networks', *IEEE Trans. Comput.*, 1985, **C-34**, pp. 934–948
2 POMBORTSIS, A., and HALATSIS, C.: 'Performance of crossbar interconnection networks in presence of hot spots', *Electron. Lett.*, 1988, **24**, pp. 182–184
3 POMBORTSIS, A., and HALATSIS, C.: 'Behaviour of circuit-switched multistage networks in presence of memory hot spot', *Electron. Lett.*, 1989, **25**, pp. 833–834
4 THOMAS, R. H.: 'Behaviour of the Butterfly parallel processor in the presence of memory hot spots'. Proc. 1986 Int. Conf. Parallel Processing, Aug. 1986, pp. 46–50

REPLY

We appreciate the concern expressed by T.-H. Lee through his comments on our letter.[1] The points of the comments are discussed below.

A processor does not independently generate at most two requests (one for the hot MM (with probability rh) and one for the background traffic (with probability $r(1-h)$) as the author claims. The assumption that a processor can independently generate and submit two requests in a network cycle is unrealistic, since each network input can only accept one request per network cycle. Instead, in Reference 1, r is the rate of request of a processor per cycle ($0 \leq r \leq 1$) and h is the probability with which a processor addresses the hot memory, given that the processor generates a request ($0 \leq h \leq 1$) (Assumptions *c* and *d*).[1] A similar set of assumptions can be found in Reference 2 where another type of nonuniformity in traffic patterns is analysed.

In a MIN the output rate of the ith stage is also the input rate to the $(i+1)$th stage. One can recursively evaluate the output rate of any stage starting with the input rate of the first stage (eqns. 1–5 in Reference 1).

In a MIN, with hot spot traffic there is a hot route leading to the hot MM. At each stage it is assumed that each connection request addresses the hot port with probability h. It must be mentioned that the formulae for P_h^i and P_{nh}^i [1] consider the uniform background traffic which is destined to one of the cool MMs obtainable from the hot port.

Generally the rate of requests at the hot port in $\alpha \times \alpha$ switch is

$$P_h = 1 - (1 - rh)^{\alpha} \quad (1)$$

caused by hot spot traffic and

$$P_u = 1 - (1 - [r(1-h)/\alpha])^{\alpha} \quad (2)$$

caused by uniform background traffic.

Hence the total rate of requests at the hot port is

$$P_h' = 1 - (1 - rh)^{\alpha}[1 - r(1-h)/\alpha]^{\alpha} \quad (3)$$

and at a cool port

$$P_{nh} = 1 - [1 - r(1 - h)/\alpha]^{\alpha} \quad (4)$$

A closer look at an $N \times N$ MIN (Fig. 1) reveals that in each stage there are N/α^i ($i = 1, 2, \ldots, n = \log_2 N$) 'hot' switching elements (SEs). The inputs of these SEs are the hot output ports of the previous stages. Thus in any input port of a particular SE there is a fraction of traffic caused by hot requests and a fraction of traffic caused by background requests which appear, as a hot request to this SE. For the hot output we apply eqn. 3 and for the cool outputs, eqn. 4. (Eqns. 4 and 5 in Reference 1.)

The analysis presented in Reference 1 allows the estimation of the request rate in any particular stage and the rate of requests at the outputs of the final stage (i.e. the bandwidth).

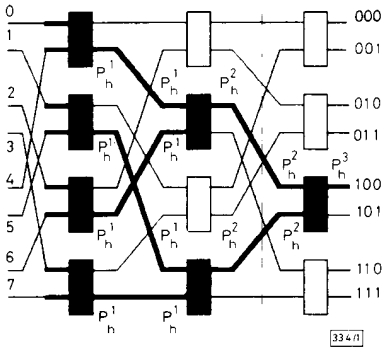

Fig. 1 *Eight port omega network leading to hot memory module*

The troughput $[S(n; r, h)]$ in the recursive algorithm presented by T.-S. Lee is dependent on the values of r'', r and the 'excess' probability $h' = x_h - x_{nh}$ in a SE at stage 1. The rate of request varies from stage to stage[2] and the fraction of hot requests in the hot route depends on the number of stage i.[3] These variations must be taken into consideration.

Many innovative computer architectures are supported by MINs. Some forms of locality of communication cause increased congestion in such networks. Under hot spot traffic, requests which address the hot MM suffer a performance degradation. This is unavoidable given the structure and the routing scheme of the MINs. What is interesting is to study switching methods and flow control procedures which minimise the performance degradation of requests which do not participate in the hot spot activity.

A. POMBORTSIS

Digital Systems and Computers Laboratory
Department of Physics
Aristotle University of Thessaloniki
54006 Thessaloniki, Greece

C. HALATSIS

Computer Laboratory
University of Athens
Panepistimiopolis, Buildings TYPA, 15771 Athens, Greece

16th January 1990

References

1 POMBORTSIS, A., and HALATSIS, C.: 'Behaviour of circuit-switched multistage networks in presence of memory hot spot', *Electron. Lett.*, 1989, **25**, pp. 833–834
2 BHUYAN, L. N.: 'An analysis of processor–memory interconnection networks', *IEEE Trans.*, 1985, **C-34**, pp. 279–283
3 KUMAR, M., and PFISTER, F. G.: 'The onset of hot spot contention'. Proc. 1986 Int. Conf. in Parallel Processing, August 1986, pp. 46–50

HIGH GAIN ERBIUM FIBRE AMPLIFIER PUMPED BY 800 nm BAND

Indexing terms: Optical fibres, Amplifiers

An optical gain as high as 30 dB is obtained at 1·5354 μm in an erbium fibre amplifier pumped in the 800 nm band. The pump power is 100 mW and the pump threshold is 27 mW. The erbium concentration is 34 ppm and the fibre length is 100 m. The maximum gain reaches 37·5 dB for a pump power of 200 mW. The pump source is a Ti : sapphire tunable laser. The most efficient pumping wavelength region is around 820 nm.

Erbium-doped fibre amplifiers are very useful for optical communication in the 1·5 μm region because of their high gain, low-insertion loss, and polarisation-insensitive gain characteristics. The pump wavelengths of the 1·48 and 0·98 μm bands are being intensively investigated since a high gain of more than 30 dB is easily obtained with laser diode pumping sources at those wavelengths.[1,2] Such high power laser diodes are not yet commercially available and their cost is high. If inexpensive pumping sources such as GaAlAs laser diodes can be used, this will be of great benefit in the field of optical communication.[3,4]

Whitely and Hodgkinson reported a gain of 8 dB at a pump wavelength of 807 nm.[5] This scheme is very interesting since GaAlAs laser diodes were utilised. The disadvantage of this pumping line is that excited state absorption (ESA) occurs. This results in relatively low gain in comparison to that obtained with 0·98 and 1·48 μm pumping wavelengths.

We show for the first time that it is possible to obtain a gain higher than 30 dB using a 800 nm band. The key to success is to use an erbium-doped fibre with a low erbium concentration. The erbium fibre has a dual shape core (inner and outer cores) where erbium ions are doped in the inner core, so that efficient pumping is realised.

The pump source for the gain measurement is a CW Ti : sapphire solid state laser pumped by an Ar ion laser. This laser is useful because it has broad tuning wavelengths from 700 to 1000 nm. The signal source is a single frequency laser diode whose wavelength can be tuned from 1·52 to 1·57 μm. The wavelength is set at 1·535 or 1·552 μm. The pump and signal beams are coupled into an erbium-doped fibre through a fibre coupler and the coupling efficiency of both beams is 96–98%. Two polarisation-insensitive optical isolators are used to suppress laser oscillation. One is installed between the coupler and the pump laser. The other is installed between the erbium-doped fibre and the output end. The erbium fibre has a relative refractive-index difference of 0·8%, a mode field diameter of 8·8 μm at 1·55 μm, an erbium concentration of 34 ppm, and an optical loss of 0·66 dB/km at 1·18 μm. The fibre has a dual shape core (high refractive-index inner core and low refractive index outer core) where the erbium ions are doped in the inner core part, so that efficient pumping is realised. The outer core diameter is 7·3 μm and the inner core diameter is 2·6 μm. The fibre is made with the VAD method and the glass composition is Er : GeO_2–SiO_2.

The optical gain at 1·5354 μm as a function of the launched pump power is shown in Fig. 1, in which the coupled signal power is −41 dBm. The pump wavelengths are 822 and 810 nm. Fibre lengths of 100 and 50 m are chosen since the doping concentration is relatively low. For the 100 m erbium fibre with an 822 nm pumping wavelength, the threshold pump power is 27 mW. When the pump power is raised to 100 mW, the gain reached 30 dB, and this increased to 34 dB for a pump power of 150 mW. The gain coefficient is estimated at 0·37 dB/mW. It is seen that the gain is strongly saturated when the pump power is larger than 100 mW. When a 50 m fibre is used, the threshold pump power decreases to 15 mW. The gains at 100 and 150 mW pump powers are 17·5 and 21 dB, respectively. At 810 nm pumping, the gain threshold is the same as that at 822 nm pumping, and the gains at 100 and 150 mW pump powers are 18 and 20 dB, respectively.

Fig. 2 shows pump wavelength dependences of the gain at 1·535 μm. The two curves with closed and open circles correspond to fibre lengths of 50 and 100 m, respectively. The launched pump power is set at 100 mW and the signal power is −42 dBm. For a fibre length of 100 m, there is a gain dip at around 810 nm which is caused by an inherent absorption peak between $^4I_{9/2}$ and $^4I_{15/2}$. That is, the absorption is too